Science Advances
AAAS

Supplementary Materials for

FOXG1 sequentially orchestrates subtype specification of postmitotic cortical projection neurons

Junhua Liu *et al*.

Corresponding author: Chunjie Zhao, zhaocj@seu.edu.cn

Sci. Adv. **8**, eabh3568 (2022)
DOI: 10.1126/sciadv.abh3568

This PDF file includes:

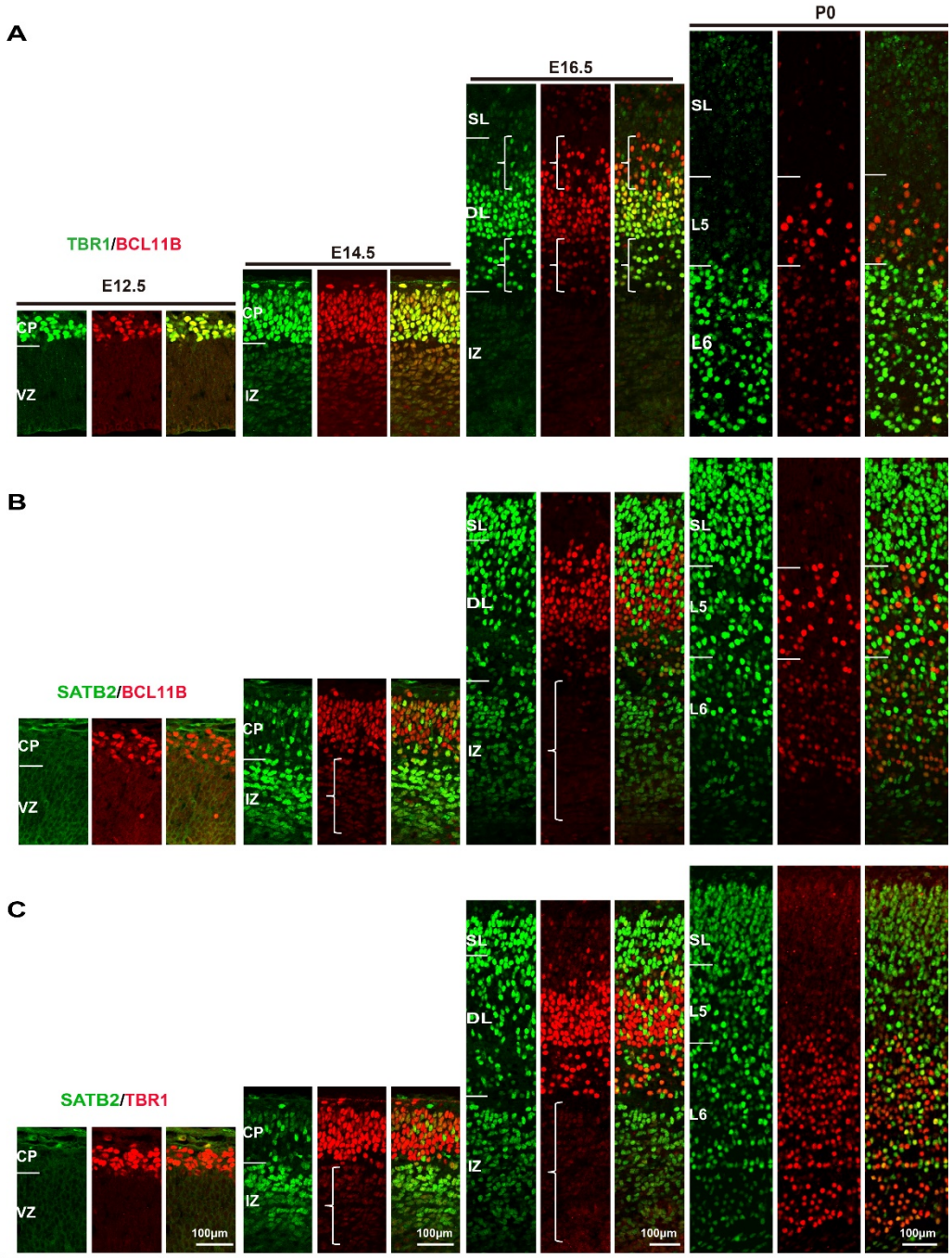

D

Subtype features of cortical projection neurons				
Subtype		Birthdate	Location	Target region
CFuN ($TBR1^{high}BCL11B^{high}$)	CThPN ($TBR1^{high}BCL11B^{low}$)	~E12.5	L6	Thalamus
	SCPN ($TBR1^{low}BCL11B^{high}$)	~E13.5	L5	spinal cord and brain stem
Deep CPN ($SATB2^{high}TBR1^{low}BCL11B^{low}$)		E12.5-E14.5	L5, L6	Controlateral cortex
Superficial CPN ($SATB2^{high}TBR1^{low}BCL11B^{-}$)		E14.5 onwards	L2-4	

Fig. S1. Dynamic expression of transcription factors defines regulatory windows during cortical neuron specification

(A) Double immunostaining against TBR1 and BCL11B from E12.5-P0 in the control cortex. At E12.5 and E14.5, TBR1 and BCL11B were both highly expressed in CFuNs. From E14.5 onward, TBR1 was gradually down-regulated in SCPNs while BCL11B was gradually down-regulated in CThPNs; by P0, SCPNs displayed a TBR^{high} $BCL11B^{low}$ pattern in layer 6 and CThPNs displayed a $BCL11B^{high}TBR1^{low}$ pattern in layer 5.

(B) Double immunostaining against SATB2 and BCL11B from E12.5-P0 in the control cortex, showing dynamic BCL11B expression during specification of deep CPNs and of superficial CPNs. At E12.5 no $SATB2^{+}$ neurons are evident. At E14.5 BCL11B is expressed at a low level in $SATB2^{high}$ deep CPNs present in the IZ. At E16.5 BCL11B was further decreased in $SATB2^{high}$ deep CPNs, which have already migrated to the CP. BCL11B was not detected in $SATB2^{high}$ superficial CPNs in the IZ. By P0, BCL11B was undetectable in most of CPNs, and only a small portion of deep CPNs retained (a low level of) BCL11B expression.

(C) Double immunostaining against SATB2 and TBR1 from E12.5-P0 in the control cortex, showing dynamic TBR1 expression during the specification of deep and superficial CPNs. Low TBR1 levels were detected in both deep and superficial CPNs throughout cortical development from E14.5-P0.

(D) Summary of the dynamic expression patterns for each cortical neuron subtype.

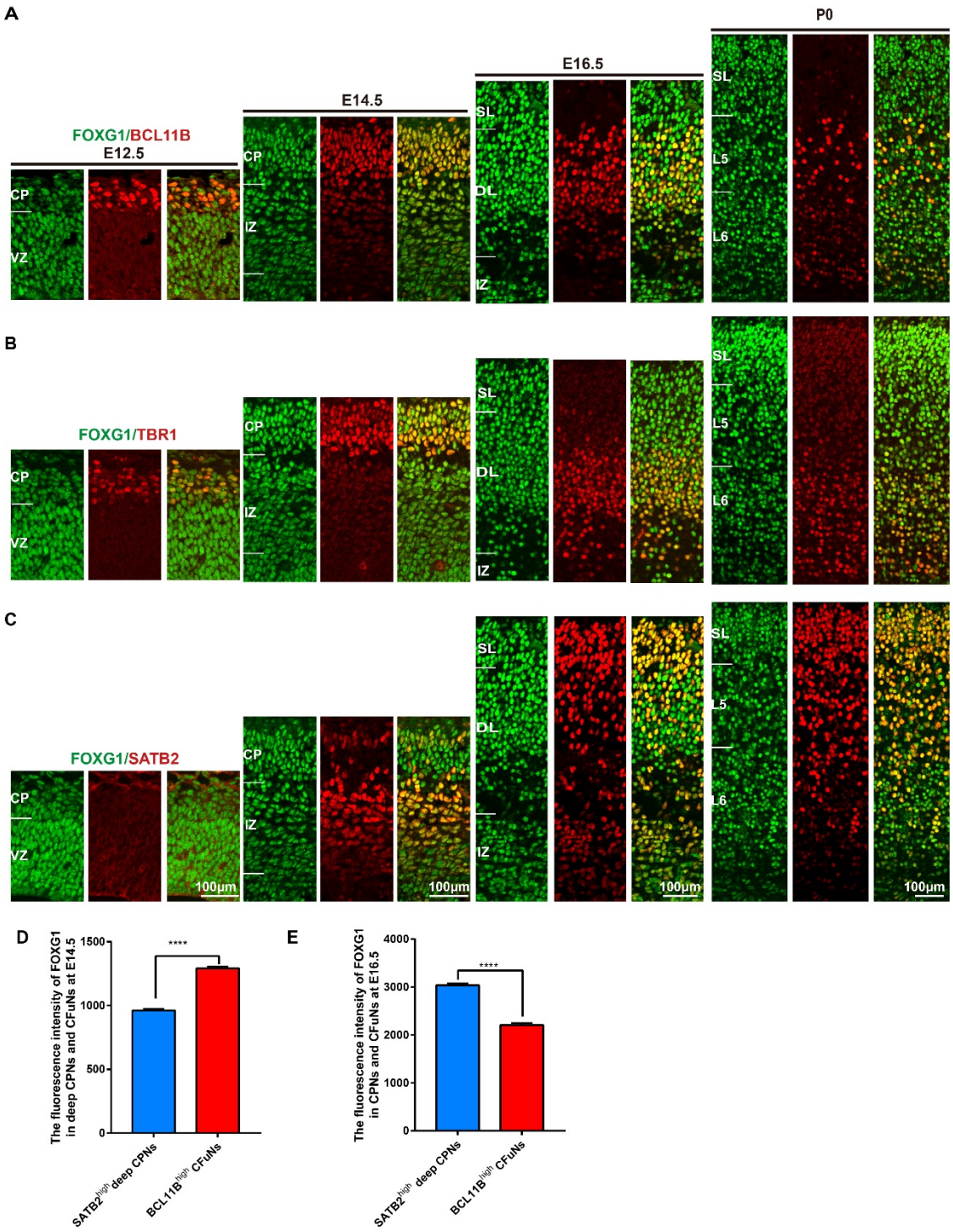
A
P0
E16.5
E14.5
FOXG1/BCL11B
E12.5
CP
VZ
IZ
DL
SL
L5
L6
B
FOXG1/TBR1
C
FOXG1/SATB2
100μm
D
The fluorescence intensity of FOXG1 in deep CPNs and CFuNs at E14.5
1500
1000
500
0
****
SATB2high deep CPNs
BCL11Bhigh CFuNs
E
The fluorescence intensity of FOXG1 in CPNs and CFuNs at E16.5
4000
3000
2000
1000
0

Fig. S2. FOXG1 expression in postmitotic cortical neurons.

(A) Double immunostaining of FOXG1 and BCL11B from E12.5-P0 in the control cortex, showing high levels of both FOXG1 and BCL11B in CFuNs and SCPNs throughout subtype specification from E12.5-P0.

(B) Double immunostaining of FOXG1 and TBR1 from E12.5-P0 in the control cortex, showing high levels of FOXG1 and TBR1 in CFuNs and CThPNs throughout subtype specification from E12.5-P0.

(C) Double immunostaining against FOXG1 and SATB2 from E12.5-P0 in the control cortex, showing FOXG1 and SATB2 expression throughout subtype specification from E12.5-E16.5.

(D) Quantification analysis of the fluorescence intensity of FOXG1 in E14.5 CP, showing that the FOXG1 level in BCL11B^{high} CFuNs is higher than SATB2^{high} CPNs.

Data are presented as the mean ± SEM, unpaired Student's t-test, ****$p < 0.0001$.

(E) Quantification analysis of the fluorescence intensity of FOXG1 in the CP at E16.5, showing that the FOXG1 level in SATB2 ^{high} CPNs is much higher than that in BCL11B^{high} CFuNs. Data are presented as the mean ± SEM, unpaired Student's t-test, ****$p < 0.0001$.

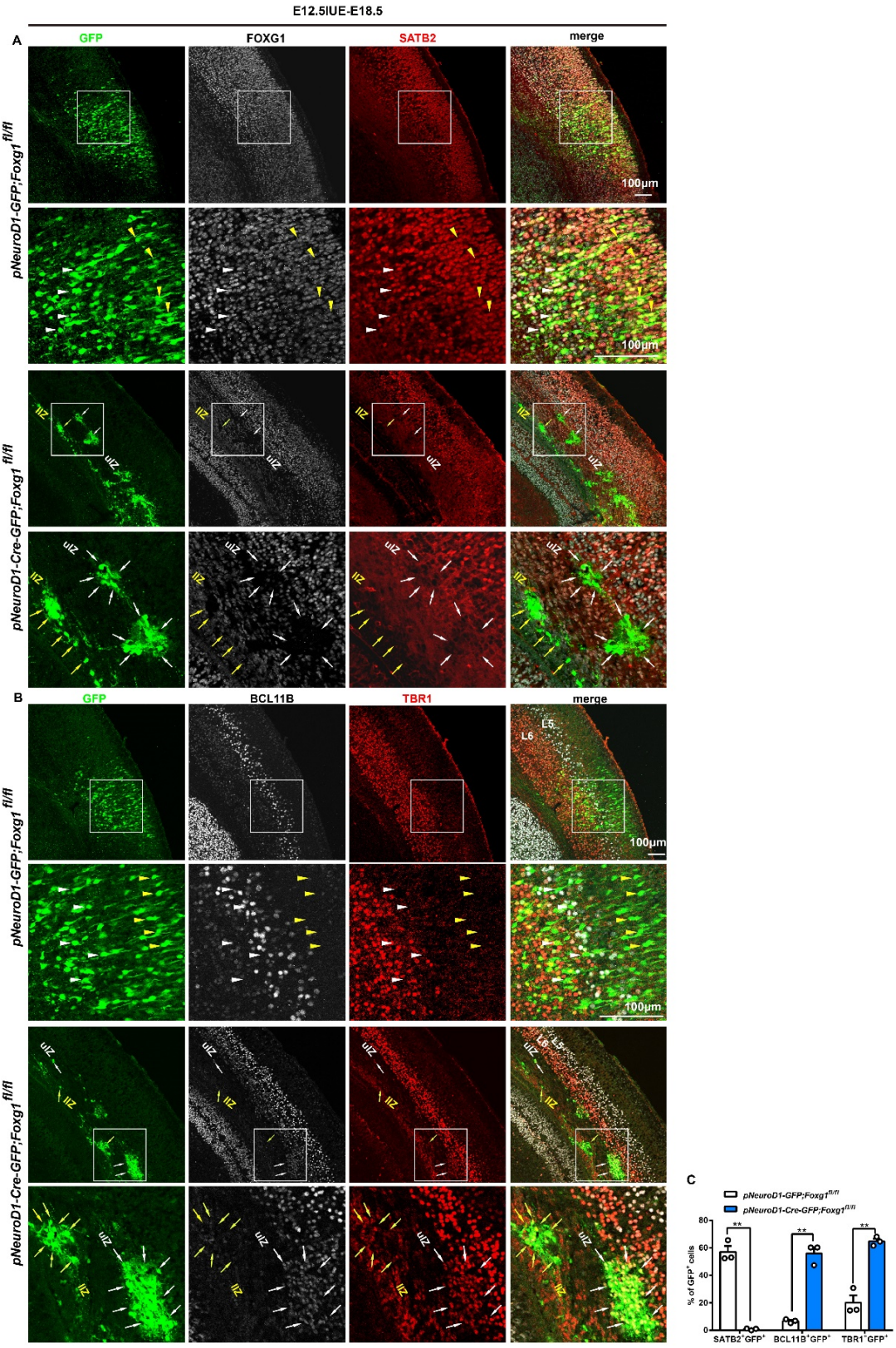
E12.5IUE-E18.5
A
GFP
FOXG1
SATB2
merge
pNeuroD1-GFP;Foxg1fl/fl
pNeuroD1-Cre-GFP;Foxg1fl/fl
100μm
uIZ
IIZ
B
GFP
BCL11B
TBR1
merge
L6
C
pNeuroD1-GFP;Foxg1fl/fl
pNeuroD1-Cre-GFP;Foxg1fl/fl
% of GFP+ cells
SATB2+GFP+
BCL11B+GFP+
TBR1+GFP+
**

Fig. S3. *Foxg1* knockdown in postmitotic neurons at E12.5 by IUE.

(A) Triple immunostaining against GFP, FOXG1, and SATB2 in the cortex at E18.5, showing that efficient FOXG1 knockdown after IUE (delivered *pNeuroD1-Cre-GFP* into the *Foxg1*$^{fl/fl}$ brains at E12.5). In the control *pNeuroD1-GFP*;*Foxg1*$^{fl/fl}$ brains, SATB2 was highly expressed in both GFP$^+$ deep CPNs (white arrowheads) and superficial CPNs (yellow arrowheads). In the *pNeuroD1-Cre-GFP*;*Foxg1*$^{fl/fl}$ brains, SATB2 was undetectable in both groups of *Foxg1*-deficient GFP$^+$ neurons, including the group near to the deep layer (white arrows) and the group arrested in the lower IZ (yellow arrows).

(B) Triple immunostaining against GFP, BCL11B, and TBR1 in the cortex at E18.5, showing the accumulation of BCL11B and TBR1 in the group of *Foxg1*-deficient GFP$^+$ neurons near to the deep layer (white arrows), and weak accumulation of TBR1 only in the group of *Foxg1*-deficient GFP$^+$ neurons arrested in the lower IZ (yellow arrows).

(C) Quantification analysis of GFP$^+$, SATB2$^+$GFP$^+$, BCL11B$^+$GFP$^+$, and TBR1$^+$GFP$^+$ neurons in cortex at E18.5, showing a remarkable decrease in the percentage of SATB2$^+$GFP$^+$/GFP$^+$ neurons; also note the obvious increase in the percentages of BCL11B$^+$GFP$^+$/GFP$^+$ and TBR1$^+$GFP$^+$/GFP$^+$ after *Foxg1* knock-down.

Data are presented as the mean ± SEM, multiple Student's t-test, with Bonferroni correction, **p < 0.01.

uIZ, upper intermediate zone; lIZ, lower intermediate zone; L5, layer 5; L6, layer 6.

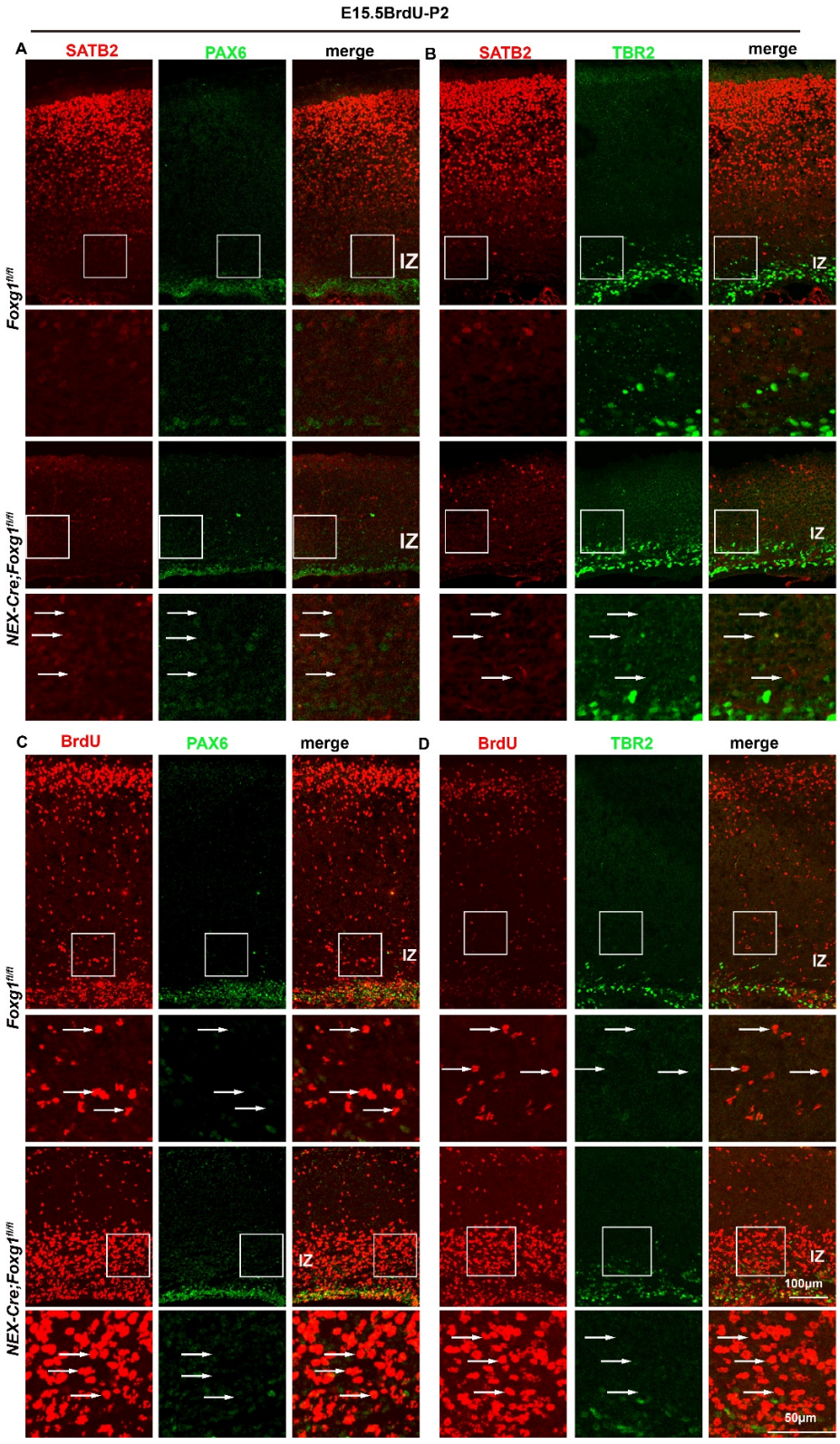
E15.5BrdU-P2
A
SATB2
PAX6
merge
B
SATB2
TBR2
merge
Foxg1fl/fl
NEX-Cre;Foxg1fl/fl
IZ
C
BrdU
PAX6
merge
D
BrdU
TBR2
merge
100μm
50μm

Fig. S4. Neurons arrested in the IZ of *NEX-Cre;Foxg1* cKO mice were SATB2^{weak} superficial CPNs but not progenitor cells.

(A) Double immunostaining of PAX6 and SATB2 at P2 cortex, showing SATB2weak neurons in the IZ did not express PAX6 in NEX-Cre;Foxg1 cKO mice (arrows).

(B) Double immunostaining of TBR2 and SATB2 at P2 cortex, showing SATB2weak neurons in the IZ did not express TBR2 in NEX-Cre;Foxg1 cKO mice (arrows).

(C) Double immunostaining of PAX6 and BrdU at P2 cortex, showing neurons labeled by E15.5 BrdU administration did not express PAX6 in both control and NEX-Cre;Foxg1 cKO mice (arrows).

(D) Double immunostaining of TBR2 and BrdU at P2 cortex, showing neurons labeled by E15.5 BrdU administration did not express TBR2 in both control and NEX-Cre;Foxg1 cKO mice (arrows).

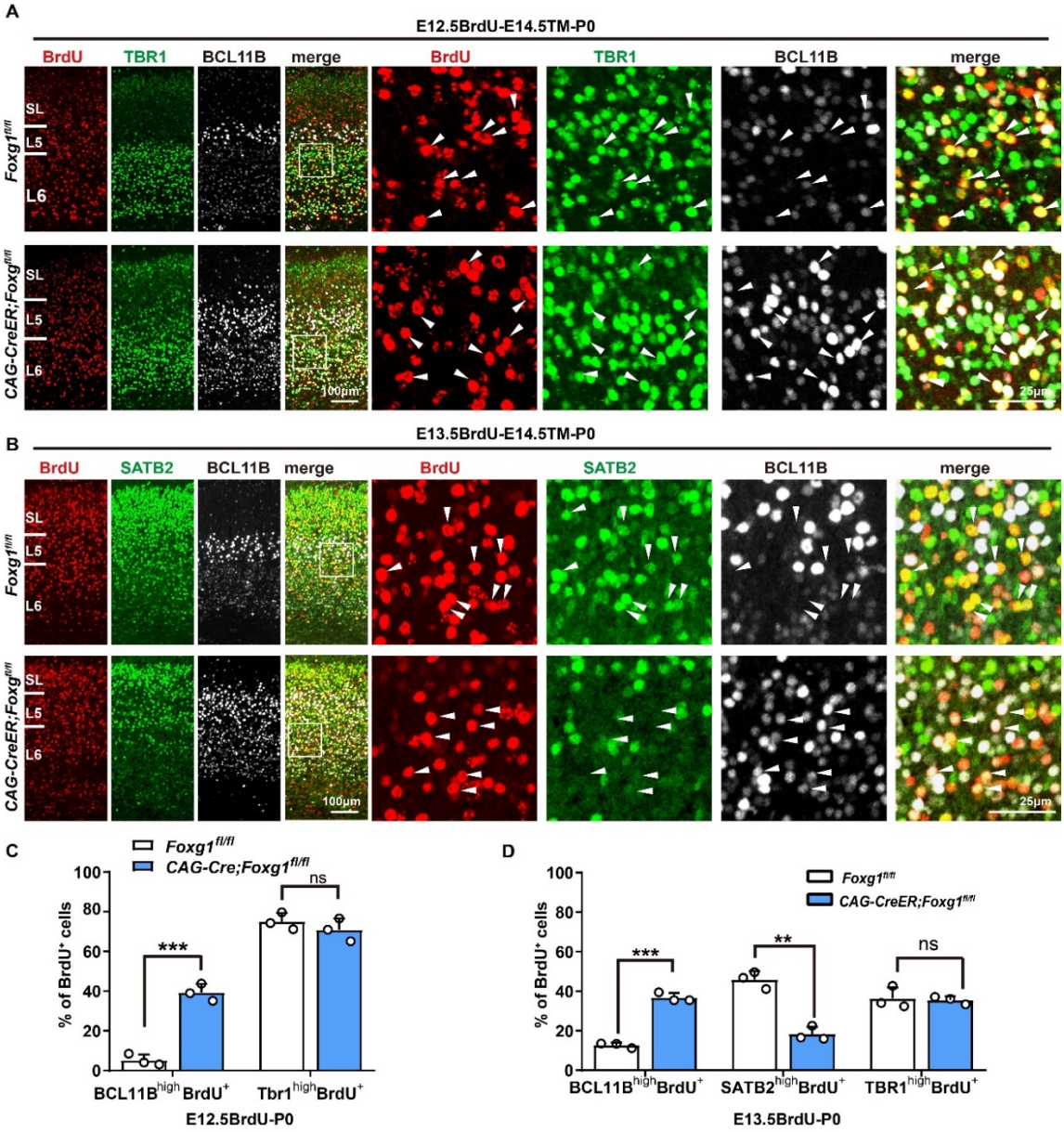
A
E12.5BrdU-E14.5TM-P0
BrdU
TBR1
BCL11B
merge
SL
L5
L6
Foxg1fl/fl
CAG-CreER;Foxg1fl/fl
100μm
25μm
B
E13.5BrdU-E14.5TM-P0
SATB2
C
Foxg1fl/fl
CAG-Cre;Foxg1fl/fl
% of BrdU+ cells
ns
***
BCL11Bhigh BrdU+
Tbr1high BrdU+
E12.5BrdU-P0
D
Foxg1fl/fl
CAG-CreER;Foxg1fl/fl
**
SATB2high BrdU+
TBR1high BrdU+
E13.5BrdU-P0

Fig. S5 Cell-tracing E12.5- and E13.5-born neurons revealed that deep CPNs develop into SCPNs in the *CAG-CreER;Foxg1* cKO cortex. Related to Fig. 2.

(A) Triple immunostaining against BrdU, TBR1, and BCL11B in P0 cortex sections, showing that most of the E12.5-born neurons displayed a $TBR1^{high}$ $BCL11B^{low}$ CThPN pattern in control mice (arrowheads), whereas BCL11B was accumulated in layer 6 $BrdU^{+}TBR1^{high}$ CThPNs in *CAG-CreER;Foxg1* cKO mice (arrowheads).

(B) Triple immunostaining against BrdU, SATB2, and BCL11B in P0 cortex sections, showing, compared to E13.5-born $BrdU^{+}$ CPNs displaying a $SATB2^{high}$ $BCL11B^{-}$ pattern in control (arrowheads), in *CAG-CreER;Foxg1* cKO cortex, most $BrdU^{+}$ neurons displayed a $BCL11B^{high}$ $SATB2^{-}$ SCPN pattern (arrowheads), indicating more E13.5-born neurons developed to SCPNs.

(C) Quantification analysis of distinct subtypes of E12.5-born neurons, showing an increased percentage of $BCL11B^{high}$ $BrdU^{+}$ /$BrdU^{+}$ neurons in; the percentage of $TBR1^{high}BrdU^{+}/BrdU^{+}$ neurons was unaffected by *Foxg1* disruption.

(D) Quantification analysis of distinct subtypes of E13.5-born neurons, showing an increased percentage of $BCL11B^{high}$ $BrdU^{+}/BrdU^{+}$ neurons, a decreased percentage of $SATB2^{high}$ $BrdU^{+}/BrdU^{+}$ neurons, and an unchanged percentage of $TBR1^{high}$ $BrdU^{+}/$ $BrdU^{+}$ neurons in *CAG-CreER;Foxg1* cKO mice.

Data are presented as the mean ± SEM, multiple Student's t-test, with Bonferroni correction, **p < 0.01; ***p < 0.001, ns: not significant.

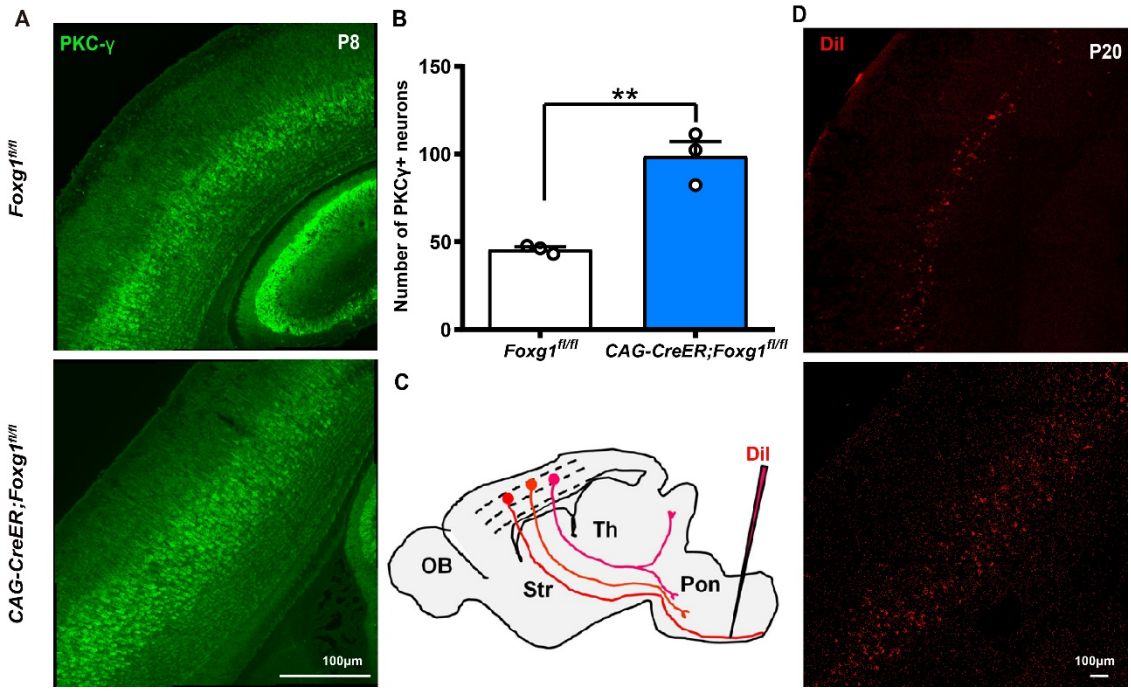

Fig. S6. Increased number of SCPNs in *CAG-CreER; Foxg1* cKO mice.

(A-B) Immunostaining against PKC-γ in the P8 cortex, showing a remarkable increase in the number of SCPNs in the *CAG-CreER;Foxg1* cKO cortex. Data are presented as the mean ± SEM, unpaired Student's t-test, $^{**}p < 0.01$.

(C) Schematic diagram for the experimental design for retrograde labelling of SCPNs via DiI injection into the *CAG-CreER;Foxg1* cKO pons at P2.

(D) DiI^{+} neurons in the P20 cortex, showing increased of SCPNs in *CAG-CreER;Foxg1* cKO mice compared to control.

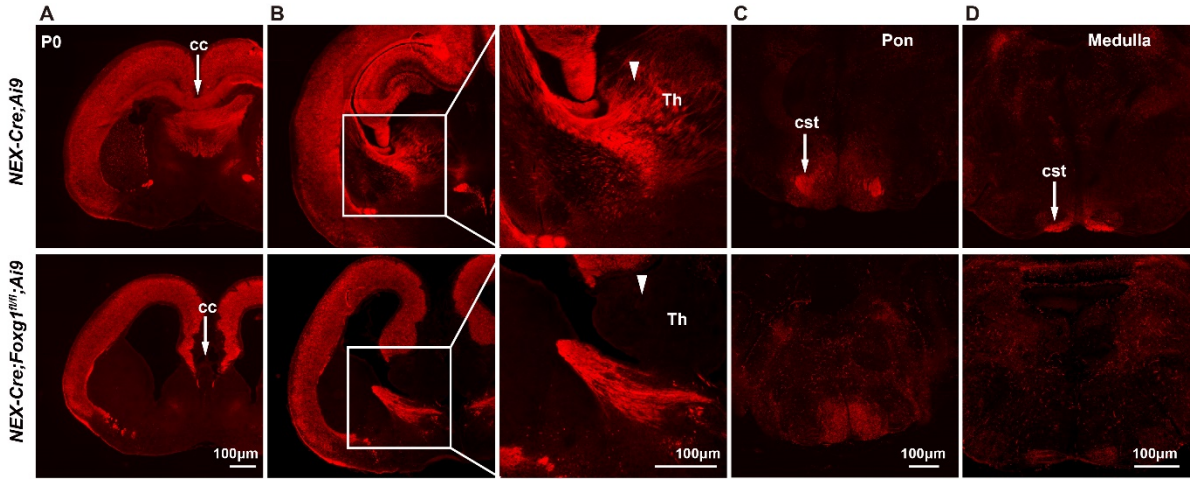

Fig. S7. Impaired corticofugal and callosal projections in *NEX-Cre;Foxg1* cKO mice at P0.

(A) Immunostaining against tdTom in P0 brains, showing normal a corpus callosum in control mice (assessed by the tdTom$^+$ signal, indicated with arrow) but the complete loss of the corpus callosum in *NEX-Cre;Foxg1* cKO mice (arrow).

(B) Immunostaining against tdTom in P0 brains, arrowheads indicates the corticothalamic projections, no corticothalamic projections were detected in *NEX-Cre;Foxg1* cKO mice.

(C) Immunostaining against tdTom in P0 brains, showing a normal corticospinal tract in control mice (arrow) but the absence of any dense tdTom$^+$ fibers in the pons of *NEX-Cre;Foxg1* cKO mice.

(D) Immunostaining against tdTom in P0 brains, showing a normal corticospinal tract in control mice (arrow) but no dense tdTom$^+$ fibers in the medulla of *NEX-Cre;Foxg1* cKO mice.

cc, corpus callosum; ic, internal capsule; cst, coticospinal tract; Th, thalamus

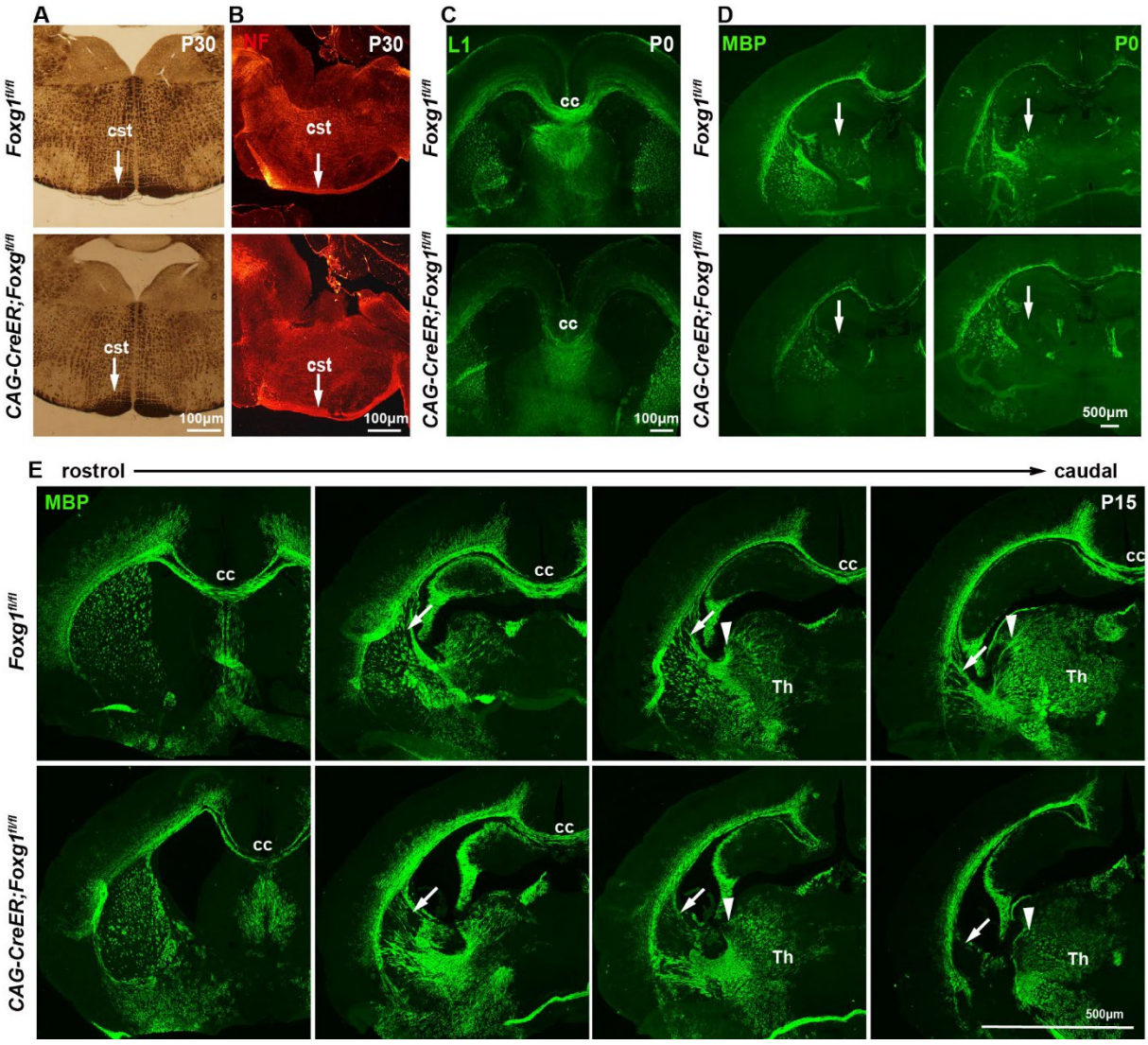
A
B
C
D
Foxg1fl/fl
CAG-CreER;Foxg1fl/fl
P30
NF
L1
P0
MBP
cst
cc
100μm
500μm
E
rostrol
caudal
Th
P15

Fig. S8. Impaired corpus callosum and subcortical projections in *CAG-CreER;Foxg1* cKO mice.

(A) Light microscopy observation of coronal sections (sequential sections spanning the brain stem) at P30 without staining, showing that *CAG-CreER;Foxg1* cKO mice have a thicker corticospinal tract (arrow) than control mice (arrow).

(B) Immunostaining against neurofilaments in sagittal sections (spanning the medulla pyramid) at P30, again showing that the corticospinal tract of *CAG-CreER;Foxg1* cKO mice (arrow) is thicker than in control mice (arrow).

(C) Immunostaining against L1 in P0 brains, showing that *CAG-CreER;Foxg1* cKO mice have very few $L1^+$ callosal fibers (arrow), unlike the normal distribution of $L1^+$ callosal fibers in control mice (arrow).

(D) Immunostaining against myelin binding protein (MBP) in P0 brains, showing that MBP^+ fibers reaching the thalamus were dramatically reduced in *CAG-CreER;Foxg1* cKO mice compared to control mice (arrows).

(E) Immunostaining against myelin binding protein (MBP) in P15 brains, showing that MBP^+ fibers in the striatum (arrowhead) and thalamus (arrow) was dramatically reduced in *CAG-CreER;Foxg1* cKO mice compared to control mice.

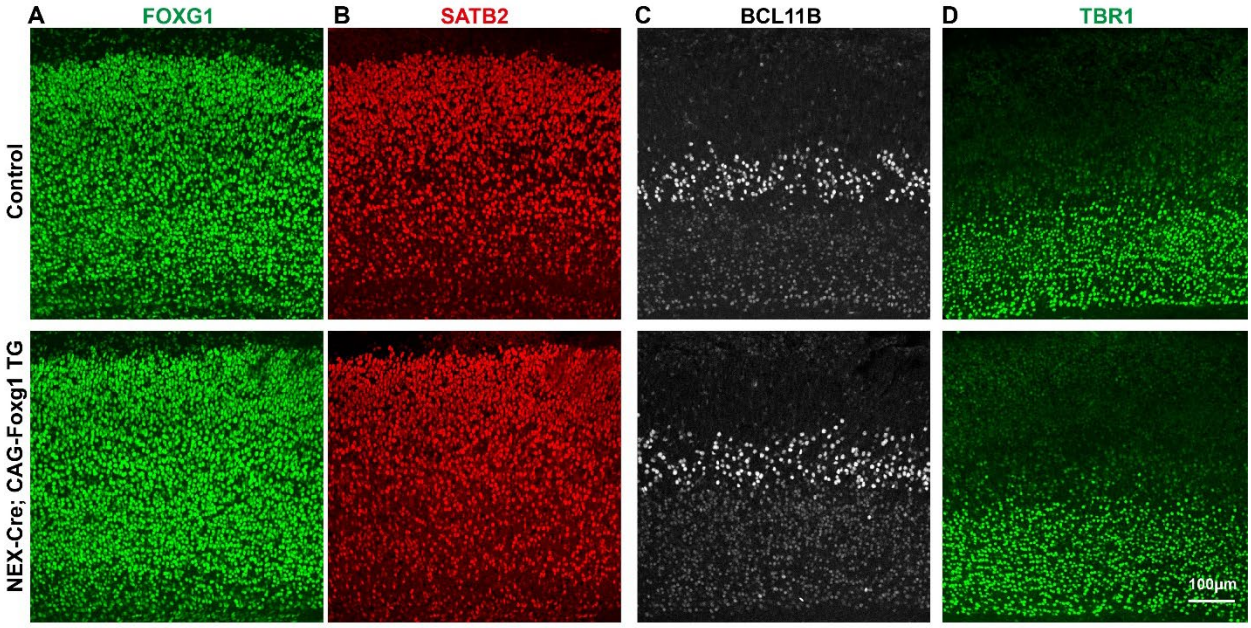
A
FOXG1
B
SATB2
C
BCL11B
D
TBR1
Control
NEX-Cre; CAG-Foxg1 TG
100μm

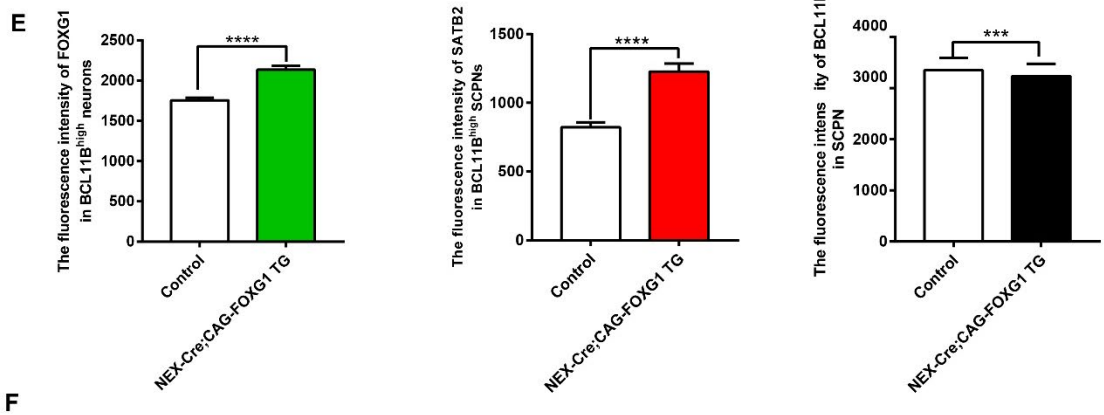
E
The fluorescence intensity of FOXG1 in BCL11B^high neurons
****
Control
NEX-Cre;CAG-FOXG1 TG
The fluorescence intensity of SATB2 in BCL11B^high SCPNs
****
Control
NEX-Cre;CAG-FOXG1 TG
The fluorescence intens ity of BCL11B in SCPN
***
Control
NEX-Cre;CAG-FOXG1 TG

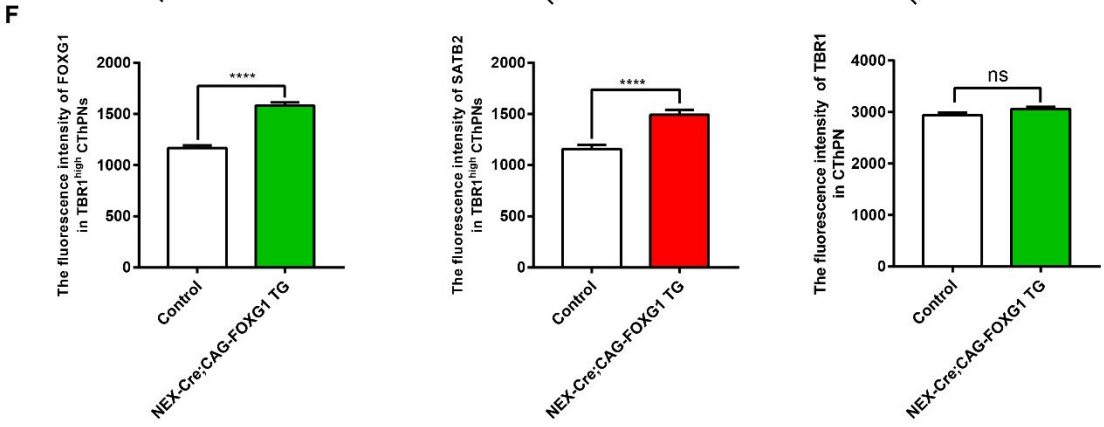
F
The fluorescence intensity of FOXG1 in TBR1^high CThPNs
****
Control
NEX-Cre;CAG-FOXG1 TG
The fluorescence intensity of SATB2 in TBR1^high CThPNs
****
Control
NEX-Cre;CAG-FOXG1 TG
The fluorescence intensity of TBR1 in CThPN
ns
Control
NEX-Cre;CAG-FOXG1 TG

Fig. S9. Overexpression of FOXG1 was able to induce SATB2 expression but was insufficient to repress *Tbr1* and *Bcl11b*.

(A) Immunostaining against FOXG1 at E18.5, showing that FOXG1 was overexpressed in *NEX-Cre;CAG-Foxg1* TG mice.

(B, C, D) Immunostaining against SATB2, BCL11B, and TBR1 at E18.5, respectively.

(E) Quantification analysis of the fluorescence intensities in $BCL11B^{high}$ SCPNs, showing the increased levels of FOXG1 and SATB2, which was accompanied with a slightly decreased level of BCL11B in *NEX-Cre;CAG-Foxg1* TG mice.

(F) Quantification analysis of the fluorescence intensities in $TBR1^{high}$ CThPNs, showing the increased levels of FOXG1 and SATB2, with an unchanged level of TBR1 in *NEX-Cre;CAG-Foxg1* TG mice.

Table S1. The antibodies for Immunofluorescence and Western blotting analyses

Rabbit anti-FOXG1	Abcam	Cat.#AB18259; RRID：AB_732415
Rabbit anti-CTIP2	Abcam	Cat.#ab28448; RRID：AB_1140055
Rat anti-CTIP2	Abcam	Cat.#ab18465; RRID：AB_2064130
Rabbit anti-TBR1	Abcam	Cat.#ab31940; RRID：AB_2200219
Rabbit anti-TBR1	Millipore	Cat.#AB10554; RRID：AB_11212765
Guinea pig anti-TBR1	Synaptic System	Cat.#328005; RRID：AB_2620072
Mouse anti-SATB2	Santa Cruz	Cat.# sc-81376; RRID：AB_1129287
Mouse anti-BrdU	Chemicon	Cat.#MAB3510; RRID：AB_94897
Rat anti-BrdU	Abcam	Cat.#ab6326; RRID：AB_305426
Chicken anti-RFP	Abcam	Cat.#ab13970; RRID：AB_300798
Rabbit anti-PKC-γ	Santa Cruz	Cat.#sc166385; RRID：AB_2018059
Rat anti-L1	Millipore	Cat.#MAB5272; RRID：AB_2133200
Mouse anti-Neurofilament	Sigma	Cat.# N5264; RRID：AB_477278
Rabbit anti-MBP	Abcam	Cat.#ab40390; RRID：AB_1141521
Rabbit anti-SOX5	Santa Cruz	Cat.#sc-20091; RRID：AB_2271083
anti-digoxigenin-alkaline phosphatase	Roche	Cat.#11093274910;RRID：AB_514497
rabbit anti-IgG	Millipore	Cat.#12-370; RRID：AB_145841

Table S2. The primers for in situ probes, qPCR and Vector construction

Mouse *Fezf2* (in situ)	F: 5'-GTGCGGCAAGGTGTTCA-3'
	R: 5'-TACAGGGCAGGAAGAACGGAC-3'
Mouse *Sox4* (in situ)	F: 5'-TACATTTATTCATGCCGGTCT-3'
	R: 5'-AGTGTTCTCCGCGTTGTTG-3'
Mouse *Sox11*(in situ)	F: 5'-GATGAAGACGACGACGAAGAT-3'
	R: 5'-CGCCTCTCAATACGTGAA-3'
Mouse *Fezf2* (qPCR)	F: 5'-CCGCCCATGTCATTCCACTT-3'
	R: 5'-GCAGCGTGTCTCTTCTGTCA-3'
Mouse *Sox5* (qPCR)	F: 5'-CGAAAACCACATTGCGGGAC-3'
	R: 5'-GAGTTAATGTGCTTGGCCACTG-3'
Mouse *Sox4* (qPCR)	F: 5'-TGGCTTCCTACCTTGCAACA-3'
	R: 5'-GGTAGCTCAGGAAAGCGACA -3'
Mouse *Sox11* (qPCR)	F: 5'-GCAGTCTGTACAAACGCTTACA-3'
	R: 5'-AGGAGGTATAAGGGAACGAGT-3'
Mouse *Satb2* (qPCR)	F: 5'-CCAGAGGACATAATGCACACCT-3'
	R: 5'-CGGGATTCCACAGAAGGCAT-3'
Mouse *Tbr1* (qPCR)	F: 5'-TGAGCAGCAGCTACCCACAT-3'
	R: 5'-GATTCGTCATCCCCCTGGTA-3'
Mouse *Ctip2* (qPCR)	F: 5'-CCAACTTTGCATCTGGCCTC-3'
	R: 5'-AGGTAACCTCCCTTGCTCTCT-3'
Mouse GAPDH (qPCR)	F: 5'-AGGTCGGTGTGAACGGATTTG-3'
	R: 5'-TGTAGACCATGTAGTTGAGGTCA-3'
Mouse *Fezf2-1* (CHIP-qPCR)	F: 5'-TGTGAGTGGCAAGGTGTAAA-3'
	R: 5'-TCTTTCCAAATGTTGGGTGAATAC-3'
Mouse *Fezf2-2* (CHIP-qPCR)	F: 5'-GCTATCCTGTTAATCTCTCATTTGT-3'
	R: 5'-CACTCAAGAACTCGGCATTTAC-3'
Mouse *Sox5* (CHIP-qPCR)	F: 5'-CAGAAACTTTGCCTGGGTTG-3'
	R: 5'-TAAACAGGCTGTCACTCACTC-3'
Mouse *Sox4* (CHIP-qPCR)	F: 5'-GTTTGGCCTACCCAGGATTTA-3'
	R: 5'-GCTATCTGTGCTGTTTGTGAAAG-3'
Mouse *Sox11* (CHIP-qPCR)	F: 5'-ACTAGCCTGAGGTGTGTAGAG-3'
	R: 5'-TCCCTCTCTGGCCTGTTT-3'
Mouse *Satb2* (CHIP-qPCR	F: 5'-CGCCTGGCAGGAAATTAAAC-3'
	R: 5'-CCTATCCCTGTGCCTCCT-3'
Mouse *Tbr1* (CHIP-qPCR)	F: 5'-CACACCACACCAGTCAGTAAG-3'
	R: 5'-CCAGTGCAAATGGGTTCTCTA-3'
Mouse *Ctip2* (CHIP-qPCR)	F: 5'-TGATCTCTGCGGTTTGCTT-3'
	R: 5'-GTAAGAGACAAACCCTCTAGGC-3'
Mouse *Tbr1* (Vector construction)	F: 5'-GAGCTCTTACGCGTGCTAGCACCATAGTACTGATTATTAGCA GTTAT CATAGC-3'
	R: 5'-AGTACCGGAATGCCAAGCTTAGCTCTAGAACCTG AACGCTGG-3'

Table S3 List of constructs carrying deletion/mutations in FOXG1-binding motifs

Construct name	Primers	Deletions/mutations
Fezf2-pro-Mut	F: 5'-TTGGGGATGATTTCAGGCAGGATAATAGAAGGC-3'	chr14:13180857-13181186 (-2477bp/-2807bp)
	R: 5'GCCTGAAATCATCCCCAAATGTTTTCTTTCTGTGGA-3'	
Fezf2-En-mut	F: 5'GGGAA ATGGGTA ACCTCAAGGCAGCTGCGTTG-3'	AT**AAA**TA→AT**GGG**TA
	R: 5'GAGGTTACCCATTTCCCAGCGTTTTCTCAAGACT-3'	
	F: 5'GACTTTTGCCCAGTCAACACAATTGATTACAAATGAGAGA-3'	TTG**TTT**A→TTG**CCC**A
	R: 5'GTTGACTGGGCAAAAGTCTAGGTCGTCTTTTCTTCCTG-3'	
Sox5-pro-mut	F: 5'AACCTGTGGGCAGGCTGTCACTCACTCTGTCCG-3'	GT**AAA**CA→GT**GGG**CA
	R: 5'CAGCCTGCCCACAGGTTTCCTTGAAGGGGCCT-3'	
Sox4-pro-Mut	F: 5'TGTGCTAGTTAACCTCTGTTTGGCAAAAAGAGT-3'	chr13:29046371-29046546 (-802bp/-978bp)
	R:5'CAGAGGTTAACTAGCACAATATCCAAAGGATAGATGGGT-3'	
Sox11-pro-Mut	F: 5'GTGTAGAGTAAGATCCTGATAATTCCACTAGTCCCGGGC-3'	chr12:28028775-28029381 (-1191bp - -1798bp)
	R: 5'CAGGATCTTACTCTACACACCTCAGGCTAGTCT-3'	
Satb2-pro-Mut	F: 5'ACTGGTCCACCTAAGGTGGCGCGGTGACTGCCC-3'	chr1:57028787-57029943 (-608bp/-1765bp)
	R: 5'CACCTTAGGTGGACCAGTCTGGCTTGGGTTTAG-3'	
Tbr1-pro-Mut	F: 5'GGTTGTGTCCTTGTTTCCAATGTGTTTCAATGGATT-3'	chr2:61639180-61639365 (-3144bp/-3330bp)
	R: 5'GGAAACAAGGACACAACCCAGAATTAAATATTT-3'	
	F: 5'CCCTCTGGATTATACTCGTGTAGTTTAAAGGTGGGGG-3'	chr2:61641477-61642017 (-492bp/-1033bp)
	R: 5'CGAGTATAATCCAGAGGGAGAGAAAAAGAACCC-3'	
Bcl11b-pre-Mut	F: 5'AACGCAAGCGCGTTAACAGGCACACAGAGATTC-3'	chr1:57028787-57029943
	R: 5'TGTTAACGCGCTTGCGTTTTCTTTGGCAGAGGC-3'	